

Positively Charged Base Surrogate for Highly Stable “Base Pairing” through Electrostatic and Stacking Interactions

Hiromu Kashida,[†] Hidehiro Ito,[†] Taiga Fujii,[†] Takamitsu Hayashi,[†] and Hiroyuki Asanuma^{*,†,‡}

Graduate School of Engineering, Nagoya University, Furocho, Chikusa-ku, Nagoya 464-8603, Japan, CREST, Japan Science and Technology Agency, 4-1-8 Honcho, Kawaguchi, Saitama 332-0012, Japan

Received February 28, 2009; E-mail: asanuma@mol.nagoya-u.ac.jp

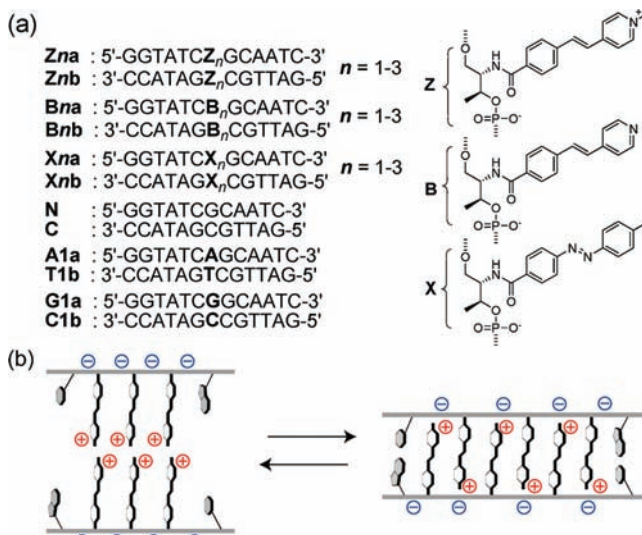
The design of new artificial nucleobases is an attractive theme in DNA chemistry. Broadly speaking, there are two trends in nucleotide design, one of which aims at biocompatible artificial nucleobases that can be substrates of enzymes, e.g., expansion of genetic alphabets.¹ The other is the design of material-oriented artificial nucleotides that do not require such biocompatibility but have excellent supramolecular properties.² In this context, there is no limitation on the components of the artificial nucleotides. Even D-ribose is not necessary as long as a sufficiently stable duplex is formed.²ⁱ

It is well-known that the addition of positively charged molecules, such as spermine or polycation, strongly stabilize the duplex.³ Hence, the incorporation of positive charges into the oligodeoxy-ribonucleotide (ODN) is an effective strategy for constructing stable duplexes at low ionic strength. Recently, Behr et al. covalently introduced oligospermine at the termini of ODNs to stabilize the duplex and control its melting temperature.⁴ However, most artificial base pairs reported so far utilize only stacking interactions and/or hydrogen bonding, and direct incorporation of positive charge on a pseudonucleobase has scarcely been investigated except for metal base pairs⁵ and oligoamine conjugates.⁴ One of the reasons is the instability of the *N*-glycosidic linkage between cationic molecules and D-ribose under acidic/basic conditions during DNA synthesis.⁶ Only a few quaternized nucleobases have been reported,⁷ although base pairs of protonated bases were widely reported so far.⁸ Accordingly, this might be the first report on the “base pairing” of quaternized molecules, which have positive charges irrespective of pH.

Previously, we described highly stable modified DNA duplex tethering neutral dyes.⁹ We found that D-threoninol is a facile but excellent acyclic scaffold for functional molecules that is compatible with natural nucleotides.¹⁰ In our design, dyes on D-threoninol were located at the counterpart of each strand to form stacked “base pairs”. These base surrogates, threoninol nucleotides, raised melting temperatures through intermolecular stacking as the number of nucleotides increased, demonstrating that dyes on D-threoninols worked as artificial “base pairs”.

In the present study, we report a new artificial cationic base surrogate with D-threoninol, which stabilizes duplexes through both electrostatic and stacking interactions. D-Threoninol has an amino residue, to which dyes can be conjugated through an amide bond. Accordingly, this linker can avoid the above-mentioned synthetic problems. Here, we incorporated *p*-methylstilbazole (**Z** in Scheme 1a) as a cationic pseudonucleobase into ODNs for further stabilization of duplexes. **Z** has a quaternized pyridine ring and a positive charge regardless of pH. Hence, a **Z**–**Z** pair should facilitate duplex formation through electrostatic interactions between the dye cation

Scheme 1^a



^a (a) Sequences of modified and native ODNs synthesized. (b) Schematic representation of stabilization by cationic “base pairs”.

and phosphate anion. In addition, **Z** has strong SHG activity¹¹ so that dye aggregates of **Z** have the potential to be applied as optical materials.

Our sequence design is depicted in Scheme 1. One to three **Z** were introduced into the counterpart of each strand. As a control, *p*-stilbazole (**B**) and *p*-methylazobenzene (**X**),¹² both of which have structures similar to that of the **Z** residue and do not have a positive charge, were introduced into ODNs.¹³ The T_m of **N/C**, the native duplex without threoninol nucleotides, was 47.7 °C under the conditions listed in Table 1.¹⁴ When one **Z**–**Z** pair was introduced into the **N/C** duplex (**Z1a/Z1b**), however, the T_m became as high as 57.7 °C. This increase with respect to the **N/C** duplex (10.0 °C) was larger than that of the **X**–**X** pair (**X1a/X1b**).¹⁵ Thus, the efficient stabilization of the duplex by incorporation of a positive charge is conclusive. It should be noted that the T_m increase was much larger than that of a natural A–T (**A1a/T1b**) or even G–C (**G1a/C1b**) pair.

Table 1. Thermodynamic Parameters of Duplexes Synthesized in This Study

sequences	T_m /°C ^a	ΔH /kcal mol ⁻¹	ΔS /cal K ⁻¹ mol ⁻¹	ΔG_{37}° /kcal mol ⁻¹	$\partial T_m / \partial \ln[\text{Na}^+]^b$	Δn_{Na^+}
Z1a/Z1b	57.7	−90.6	−246	−14.1	3.7	1.7
X1a/X1b	53.3	−86.2	−238	−12.3	4.3	1.9
N/C	47.7	−89.9	−254	−11.2	4.6	2.1
A1a/T1b	49.4	−94.0	−266	−11.6	4.7	2.4
G1a/C1b	53.4	−100.5	−282	−13.1	4.5	2.4

^a [ODN] = 5 μM, [NaCl] = 100 mM, pH 7.0 (10 mM phosphate buffer). ^b [ODN] = 2 μM, pH 7.0 (10 mM phosphate buffer).

[†] Nagoya University.

[‡] Japan Science and Technology Agency.

To evaluate the effect of positive charge on the T_m thermodynamically, the Gibbs free energy, enthalpy, and entropy changes upon duplex formation were determined from $1/T_m$ versus $\ln(C_T/4)$ plots as listed in Table 1.¹⁶ The $-\Delta G_{37}^{\circ}$ of **X1a/X1b** without a positive charge was 12.3 kcal mol⁻¹, which was 1.1 kcal mol⁻¹ more stable than **N/C**.¹⁷ However, **Z1a/Z1b** was even more stable than **X1a/X1b**: $-\Delta G_{37}^{\circ}$ of **Z1a/Z1b** was as high as 14.1 kcal mol⁻¹. $-\Delta H$ of **Z1a/Z1b** was 4.4 kcal mol⁻¹ larger than that of **X1a/X1b**, indicating that a positive charge on the **Z** residue exothermically stabilized the duplex due to electrostatic interaction.^{18,19} $-\Delta G_{37}^{\circ}$ of **Z1a/Z1b** was even larger than those of **A1a/T1b** and **G1a/C1b**, clearly demonstrating that the **Z-Z** pair stabilized the duplex much more than native base pairs did (**A-T** and **G-C**).

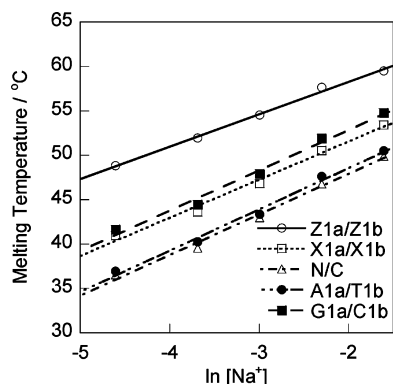


Figure 1. Dependence of T_m s of **Z1a/Z1b**, **X1a/X1b**, **N/C**, **A1a/T1b**, and **G1a/C1b** on salt concentration. [ODN] = 2 μM , pH 7.0 (10 mM phosphate buffer).

Figure 1 shows linear plots of T_m with respect to logarithmic salt concentrations, whose slope gives the number of cations released upon duplex dissociation (Δn_{Na^+}).²⁰ As summarized in Table 1, Δn_{Na^+} of **Z1a/Z1b** was 1.7 (per duplex) whereas Δn_{Na^+}

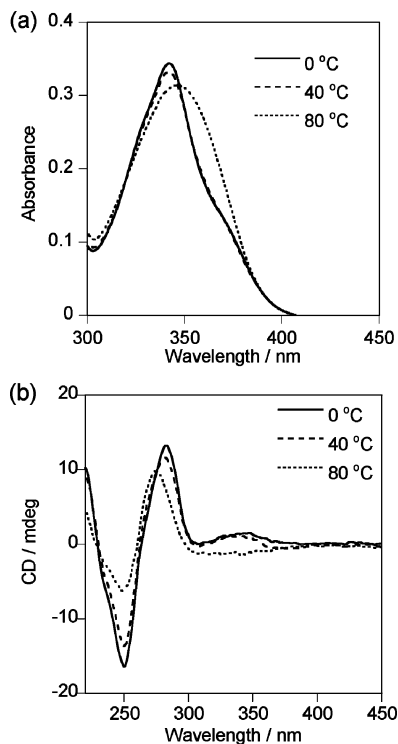


Figure 2. (a) UV-vis and (b) CD spectra of **Z1a/Z1b** at 80, 40, and 0 °C. [ODN] = 5 μM , [NaCl] = 100 mM, pH 7.0 (10 mM phosphate buffer).

Table 2. Effect of Dye Number on Melting Temperatures

n	$T_m / ^\circ\text{C}^a$		
	Zna/Znb	Bna/Bnb	Xna/Xnb
0		47.7	
1	57.7	52.7	53.3
2	66.2	50.9	54.8
3	68.5	50.6	57.7

^a [ODN] = 5 μM , [NaCl] = 100 mM, pH 7.0 (10 mM phosphate buffer).

of **X1a/X1b** and **N/C** were 1.9 and 2.1, respectively: fewer cations were released from **Z1a/Z1b** upon dissociation, indicating that the electrostatic repulsion between phosphate anions was lessened by cationic dyes.²¹

UV-vis and CD spectra of **Z1a/Z1b** revealed the stacked structure of the **Z-Z** pair in the duplex (see Figure 2).²² At 0 °C where duplexes were completely formed, a peak at ~ 340 nm in the UV-vis spectrum shifted to a shorter wavelength and became narrower (see Figure 2a). This hypsochromic shift and narrowing of the band demonstrated that two **Z** residues were stacked antiparallel along the helical axis in the DNA double helix.²³ The coincidence of the T_m at 360 nm (58.8 °C) with that at 260 nm also supports the hypothesis that **Z-Z** stacking was associated with duplex formation (see Supporting Information for melting profiles). As expected, CD was also induced at ~ 360 nm by lowering the temperature (see Figure 2b). However, its intensity was rather weak indicating that the **Z-Z** pair did not wind strongly, because the threoninol scaffold allowed a firmly stacked, unwound ladder-like structure due to its flexibility.⁹

Further introduction of cationic dyes greatly stabilized the duplex. Table 2 shows the melting temperatures of **Zna/Znb**, **Bna/Bnb**, and **Xna/Xnb**. T_m monotonically increased when the number of **Z-Z** pairs in the duplex increased from one to three. In particular, the T_m of **Z3a/Z3b** was 68.5 °C, which was as much as 20 °C higher compared with **N/C** (see Figure 3). The melting temperature of **Z3a/Z3b** increased as the concentration of the duplex increased (see Supporting Information). In addition, single-stranded **Z3a** and **Z3b** did not show such hypochromicity, demonstrating that the sigmoid curve of **Z3a/Z3b** was unambiguously derived from their hybridization.²⁴ These results clearly show that multiple incorporation of **Z-Z** pairs did not destabilize but instead largely stabilized the duplex. It should be noted that accumulated positive charges did not act repulsively but facilitated assembly.²⁵ On the other hand, incorporation of multiple **X-X** pairs showed less stabilization. The T_m of **X3a/X3b** was ~ 10 °C higher than that of the **N/C** duplex

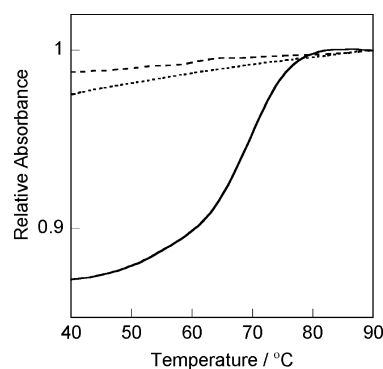


Figure 3. Melting profiles of **Z3a/Z3b** (solid line), single-stranded **Z3a** (broken line), and **Z3b** (dotted line) by monitoring absorbance at 260 nm. Melting profiles were normalized by the absorbance at 90 °C. [ODN] = 5 μM , [NaCl] = 100 mM, pH 7.0 (10 mM phosphate buffer).

but 10 °C lower than that of **Z3a/Z3b**. Furthermore, the multiple introduction of *p*-stilbazole (**B**) residues did not raise the T_m at all. Taken together, these results clearly demonstrate that a positive charge on the dye crucially contributes to the enhanced stabilization of the duplex.

In conclusion, cationic “base pairs” were successfully incorporated into an ODN. This “base pair” strongly stabilized duplexes by electrostatic interactions as well as stacking interactions. Further stabilization was observed by multiplying the dye number. Due to this large stabilization, the preparation of dye aggregates without the assistance of natural bases is promising. This design might allow for new double helical motifs that are completely different from the natural duplex.²⁶

Acknowledgment. This work was supported by Core Research for Evolution Science and Technology (CREST), Japan Science and Technology Agency (JST). Partial support by a Grant-in-Aid for Scientific Research from the Ministry of Education, Culture, Sports, Science and Technology, Japan and The Mitsubishi Foundation (for H.A.) is also acknowledged.

Supporting Information Available: Experimental procedures of the preparation of modified ODNs and spectroscopic measurements, UV and CD spectra and melting profiles of duplexes, energy-minimized structures of dyes and **X1a/X1b**. This material is available free of charge via the Internet at <http://pubs.acs.org>.

References

- (1) (a) Hirao, I. *Curr. Opin. Chem. Biol.* **2006**, *10*, 622–627. (b) Kool, E. T. *Curr. Opin. Chem. Biol.* **2000**, *4*, 602–608, references therein.
- (2) (a) Gao, J.; Strässler, C.; Tahmassebi, D.; Kool, E. T. *J. Am. Chem. Soc.* **2002**, *124*, 11590–11591. (b) Brotschi, C.; Leumann, C. J. *Angew. Chem.* **2003**, *115*, 1694–1697; *Angew. Chem., Int. Ed.* **2003**, *42*, 1655–1658. (c) Tanaka, K.; Tengeji, A.; Kato, T.; Toyama, N.; Shionoya, M. *Science* **2003**, *299*, 1212–1213. (d) Minakawa, N.; Kojima, N.; Hikishima, S.; Sasaki, T.; Kiyosue, A.; Atsumi, N.; Ueno, Y.; Matsuda, A. *J. Am. Chem. Soc.* **2003**, *125*, 9970–9982. (e) Lai, J. S.; Kool, E. T. *J. Am. Chem. Soc.* **2004**, *126*, 3040–3041. (f) Dohno, C.; Okamoto, A.; Saito, I. *J. Am. Chem. Soc.* **2005**, *127*, 16681–16684. (g) Nakamura, M.; Ohtoshi, Y.; Yamana, K. *Chem. Commun.* **2005**, 5163–5165. (h) Mayer-Enthart, E.; Wagenknecht, H.-A. *Angew. Chem.* **2006**, *118*, 3451–3453; *Angew. Chem., Int. Ed.* **2006**, *45*, 3372–3375. (i) Malinovsky, V. L.; Samain, F.; Häner, R. *Angew. Chem.* **2007**, *119*, 4548–4551; *Angew. Chem., Int. Ed.* **2007**, *46*, 4464–4467. (j) Tawarada, R.; Seio, K.; Sekine, M. *J. Org. Chem.* **2008**, *73*, 383–390.
- (3) Tabor, H. *Biochemistry* **1962**, *1*, 496–501.
- (4) (a) Pons, B.; Kotera, M.; Zuber, G.; Behr, J.-P. *ChemBioChem* **2006**, *7*, 1173–1176. (b) Noir, R.; Kotera, M.; Pons, B.; Remy, J.-S.; Behr, J.-P. *J. Am. Chem. Soc.* **2008**, *130*, 13500–13505.
- (5) Recently, many “metal base pairs”, which stabilize a duplex by metal coordination, have been reported: Clever, G. H.; Kaul, C.; Carell, T. *Angew. Chem., Int. Ed.* **2007**, *46*, 6226–6236.
- (6) (a) Lindahl, T. *Nature* **1993**, *362*, 709–715. (b) Huber, R.; Amann, N.; Wagenknecht, H.-A. *J. Org. Chem.* **2004**, *69*, 744–751.
- (7) (a) Ezaz-Nikpay, K.; Verdine, G. L. *J. Am. Chem. Soc.* **1992**, *114*, 6562–6563. (b) Onyemauwa, F. O.; Schuster, G. B. *Org. Lett.* **2006**, *8*, 5255–5258. (c) Lee, S.; Bowman, B. R.; Ueno, Y.; Wang, S.; Verdine, G. L. *J. Am. Chem. Soc.* **2008**, *130*, 11570–11571.
- (8) Frank-Kamenetskii, M. D. *Methods Enzymol.* **1992**, *211*, 180–191.
- (9) Kashida, H.; Fujii, T.; Asanuma, H. *Org. Biomol. Chem.* **2008**, *6*, 2892–2899.
- (10) (a) Asanuma, H.; Shirasuka, K.; Takarada, T.; Kashida, H.; Komiyama, M. *J. Am. Chem. Soc.* **2003**, *125*, 2217–2223. (b) Asanuma, H.; Liang, X. G.; Nishioka, H.; Matsunaga, D.; Liu, M.; Komiyama, M. *Nat. Protocols* **2007**, *2*, 203–212.
- (11) Duan, X.-M.; Konami, H.; Okada, S.; Oikawa, H.; Matsuda, H.; Nakanishi, H. *J. Phys. Chem.* **1996**, *100*, 17780–17785.
- (12) Nishioka, H.; Liang, X. G.; Kashida, H.; Asanuma, H. *Chem. Commun.* **2007**, 4354–4356.
- (13) Schemes for synthesis of phosphoramidite monomer containing these dyes are depicted in the Supporting Information. All modified ODNs listed in Scheme 1a were purified by reversed-phase HPLC and characterized by MALDI-TOF mass spectrometry. *MALDI-TOF mass spectrometry*: **Z1a**: Obsd m/z 4033 (Calcd for [**Z1a**+H⁺]: m/z 4034); **Z1b**: Obsd m/z 4033 (Calcd for [**Z1b**+H⁺]: m/z 4034); **Z2a**: Obsd m/z 4423 (Calcd for [**Z2a**+H⁺]: m/z 4423); **Z2b**: Obsd m/z 4423 (Calcd for [**Z2b**+H⁺]: m/z 4423); **Z3a**: Obsd m/z 4813 (Calcd for [**Z3a**+H⁺]: m/z 4812); **Z3b**: Obsd m/z 4810 (Calcd for [**Z3b**+H⁺]: m/z 4812); **B1a**: Obsd m/z 4019 (Calcd for [**B1a**+H⁺]: m/z 4019); **B1b**: Obsd m/z 4019 (Calcd for [**B1b**+H⁺]: m/z 4019); **B2a**: Obsd m/z 4392 (Calcd for [**B2a**+H⁺]: m/z 4393); **B2b**: Obsd m/z 4393 (Calcd for [**B2b**+H⁺]: m/z 4393); **B3a**: Obsd m/z 4767 (Calcd for [**B3a**+H⁺]: m/z 4767); **B3b**: Obsd m/z 4768 (Calcd for [**B3b**+H⁺]: m/z 4767). **X1a**: Obsd m/z 4034 (Calcd for [**X1a**+H⁺]: m/z 4034); **X1b**: Obsd m/z 4034 (Calcd for [**X1b**+H⁺]: m/z 4034); **X2a**: Obsd m/z 4424 (Calcd for [**X2a**+H⁺]: m/z 4423); **X2b**: Obsd m/z 4423 (Calcd for [**X2b**+H⁺]: m/z 4423); **X3a**: Obsd m/z 4813 (Calcd for [**X3a**+H⁺]: m/z 4812); **X3b**: Obsd m/z 4813 (Calcd for [**X3b**+H⁺]: m/z 4812).
- (14) Melting curves of duplex DNA were obtained with a Shimadzu UV-1800 by measuring the change of absorbance at 260 nm versus temperature (unless otherwise noted). The melting temperature (T_m) was determined from the maximum in the first derivative of the melting curve. Both the heating and cooling curves were measured, and the T_m measurements obtained from them coincided with each other within 2.0 °C. The temperature ramp was 0.5 °C min⁻¹.
- (15) The size of **X** is virtually identical to that of **Z**. See Supporting Information for energy-minimized structures of **Z** and **X**.
- (16) Thermodynamic parameters of duplex (ΔH , ΔS) were determined from $1/T_m$ versus $\ln(C_T/4)$ plots by the following equation: $1/T_m = R/\Delta H \ln(C_T/4) + \Delta S/\Delta H$, where C_T is the total concentration of ODNs. ΔG_{37}° was calculated from the ΔH and ΔS values. The number of sodium ions released upon duplex dissociation (Δn_{Na^+}) was determined from a T_m versus $\ln[Na^+]$ plot by the following equation: $\Delta n_{Na^+} = -1.11(\Delta H/RT_m^2) \partial T_m / \partial \ln[Na^+]$, where $\partial T_m / \partial \ln[Na^+]$ is the slope of the line in Figure 1. The T_m value at a total oligomer strand concentration of 4 μ M in the presence of 100 mM NaCl was used. ΔH was determined from a $1/T_m$ versus $\ln(C_T/4)$ plot. Errors of ΔH , ΔS , ΔG_{37}° , and Δn_{Na^+} were estimated to be 4%, 4%, 1%, and 7%, respectively.
- (17) We calculated thermodynamic parameters by assuming heat capacity change (ΔC_p) to be zero. However, ΔC_p might affect thermodynamic parameters: (a) Wu, P.; Nakano, S.; Sugimoto, N. *Eur. J. Biochem.* **2002**, *269*, 2821–2830. (b) Tikhomirova, A.; Taulier, N.; Chalikian, T. V. *J. Am. Chem. Soc.* **2004**, *126*, 16387–16394.
- (18) In the case of **Z1a/Z1b**, enhanced stacking interaction between **Zs** and neighboring GC base pairs due to the electron donation from GC to **Zs** might also contribute to the stability. See: Reha, D.; Kabeláč, M.; Ryjáček, F.; Šponer, J.; Šponer, J. E.; Elstner, M.; Suhai, S.; Hobza, P. *J. Am. Chem. Soc.* **2002**, *124*, 3366–3376.
- (19) Incorporation of two and three **Z-Z** pairs (**Z2a/Z2b** and **Z3a/Z3b**) drastically increased $-\Delta H$ and $-\Delta G_{37}^{\circ}$. See Supporting Information for the thermodynamic parameters.
- (20) (a) Record Jr, M. T.; Anderson, C. F.; Lohman, T. M. *Q. Rev. Biophys.* **1978**, *11*, 103–178. (b) Nakano, S.; Fujimoto, M.; Hara, H.; Sugimoto, N. *Nucleic Acids Res.* **1999**, *27*, 2957–2965. (c) Soto, A.; M.Kankia, B. I.; Dande, P.; Gold, B.; Marky, L. A. *Nucleic Acids Res.* **2002**, *30*, 3171–3180.
- (21) Δn_{Na^+} of **X1a/X1b** was lower than those of **A1a/T1b** and **G1a/C1b**, indicating electrostatic repulsion was relieved in this duplex although **X** has no positive charges. The small Δn_{Na^+} may be caused by the stretched structure of **X1a/X1b**, where distances between phosphates were lengthened by the introduced **X-X** pair. See Supporting Information for energy-minimized structure of **X1a/X1b** calculated by InsightII/Discover 3.
- (22) The UV/vis spectra and CD spectra were measured on JASCO model V-560 and JASCO model J-820 instruments with 10-mm quartz cells, respectively. Both were equipped with programmed temperature controllers.
- (23) Kasha, M. *Radiat. Res.* **1963**, *20*, 55–70.
- (24) The melting profile of **Z2a/Z2b** also exhibited a similar sigmoid curve. See Supporting Information.
- (25) Incorporation of multiple **Z-Z** pairs further stabilized the duplex by electrostatic interaction. Δn_{Na^+} of **Z2a/Z2b** decreased compared with **Z1a/Z1b**, whereas that of **X2a/X2b** was much larger than that of **X1a/X1b**. See Supporting Information for thermodynamic parameters of **Z2a/Z2b** and **X2a/X2b**.
- (26) Furusho, Y.; Yashima, E. *Chem. Rec.* **2007**, *7*, 1–11.

JA9013002